

PACS numbers: 42.81.Cn; 42.70.Nq
DOI: 10.1070/QE2003v033n03ABEH002401

Photosensitivity of germanosilicate fibres and preforms doped with nitrogen inhomogeneously over the cross section

Yu.P. Yatsenko, V.M. Mashinsky, O.I. Medvedkov, O.D. Sazhin,
E.M. Dianov, V.F. Khopin, N.N. Vechkanov, A.N. Gur'yanov

Abstract. **The effect of the inhomogeneous distribution of nitrogen impurity on the photosensitivity of germanosilicate fibres is studied. For this purpose, single-mode fibres with different alternations of the core layers sintered in nitrogen and oxygen atmospheres were specially prepared by the MCVD technique. Photoinduced variations in the quadratic nonlinear susceptibility and refractive index of these fibres were recorded. It is shown that the recording efficiency depends on the radial distribution of germanium oxygen-deficient centres, which can be controlled at the stage of sintering through a nonuniform doping by nitrogen over the cross-section.**

Keywords: *germanosilicate optical fibres, point defects, photoinduced quadratic nonlinear susceptibility, photorefractive effect*.

1. Introduction

Doping of germanosilicate fibres with nitrogen even in quite insignificant concentrations (less than 0.1 %) raises the efficiency of recording photoinduced gratings of the refractive index Δn and a quadratic nonlinear susceptibility $\chi^{(2)}$ [1, 2]. Such an influence of nitrogen can be attributed to the fact that it creates additional stable traps of photoelectrons in the glass structure during photoionisation of the germanium oxygen-deficient centres (GODCs) [3]. Besides, polyvalent nitrogen atoms can modify the nearest surrounding of the GeE' centres responsible for the photosensitivity of fibres in both effects [2]. In this case, the photosensitivity of glass can be improved due to the formation of additional bonds with photoionised GODCs that cause the passivation of positive charges and prevent their recombination with photoelectrons.

On the other hand, an alternative explanation for the increase in photosensitivity that is not related to the modification of photocentres by nitrogen can be offered in view of a very low concentration of nitrogen in the series of fibres investigated by us in Refs [1, 2]. Sintering and collapse of preforms in nitrogen atmosphere may result not only in an increase in the concentration of GODCs, but also in their inhomogeneous distribution due to the diffusion of germanium and nitrogen. The inhomogeneous radial distribution of GODCs, which are the main donor photocentres in germanosilicate glass, may influence considerably the charge transfer processes (photoionisation, charge separation and recombination). These processes are significant mainly for the formation of the $\chi^{(2)}$-grating structure, but may also play an important role for initiating processes occurring at the final stage of formation of the Bragg grating.

In this connection, it would be appropriate to remark that the currently available literature does not provide a clear picture of the role played by the radial GODC distribution in increasing the photosensitivity of germanosilicate fibres by their doping with some other impurities like phosphorus, boron and tin. For example, doping of germanosilicate glass with phosphorus has a favourable influence on the efficiency of recording of the photoinduced $\chi^{(2)}$ grating [4]. At the same time, it suppresses strongly GODCs with an absorption band at 242 nm [5].

In this work, we studied the photosensitivity of the fibres prepared by us with a core containing layers sintered in an atmosphere of nitrogen or oxygen. A comparison with the standard fibres enabled us to isolate the contribution of the inhomogeneous distribution of GODCs in the mechanism of formation of the $\chi^{(2)}$ grating and of the photoinduced refractive index in germanosilicate glass.

2. Samples

Single-mode fibres were prepared using the MCVD technique in which core layers were sintered in an atmosphere of O_2 or N_2O at identical flow rates of silicon and germanium chlorides. The deposition of the porous glass layer and its sintering in oxygen were carried out during a single pass of the burner (standard regime), while the layer with nitrogen was prepared during two passes. In the first pass, the porous glass layer was deposited in oxygen by lowering the temperature, while the melting (sintering) of this layer was carried out in an atmosphere of N_2O during the second pass. The core of one of the fibres (No. 913) was sintered completely in nitrogen atmosphere. The core of fibre No. 909 was sintered only in standard oxygen atmosphere. Two types of fibres were prepared with

Yu.P. Yatsenko D.V. Skobeltsyn Institute of Nuclear Physics, M.V. Lomonosov Moscow State University, Vorob'evy gory, 119992 Moscow, Russia;
V.M. Mashinsky, O.I. Medvedkov, O.D. Sazhin, E.M. Dianov Fiber Optics Research Center, A.M. Prokhorov General Physics Institute, Russian Academy of Sciences, ul. Vavilova 38, 119991 Moscow, Russia;
V.F. Khopin, N.N. Vechkanov, A.N. Gur'yanov Institute of Chemistry of High-Purity Substances, Russian Academy of Sciences, ul. Tropinina 49, 603950 Nizhny Novgorod, Russia

Received 19 June 2002
Kvantovaya Elektronika **33** (3) 275–280 (2003)
Translated by Ram Wadhwa

Table 1. Experimental Samples.

Sample No.	Molar concentration of GeO_2 in the core (%)	Sintering and collapse atmosphere	Absorption coefficient at $\lambda = 242$ nm/ dB mm^{-1}	Absorption coefficient at $\lambda = 266$ nm/ dB mm^{-1}	Cut-off wavelength/nm	$\frac{I_2}{I_1^2}/10^{-14}$ W^{-1} cm^2
909	6.5	O_2	215	9	830	2.7
913	7.5	N_2O	380	15	830	5.9
916	8.5	O_2, N_2O	415	18	820	7.5
917	8	N_2O, O_2	345	14	855	2.4

a double-layer core. In one of them (fibre No. 916), the inner core layer was prepared in an atmosphere of N_2O, while the peripheral core layer was prepared in an atmosphere of O_2. The core preparation in another fibre (No. 917) was carried out in the reverse order, i.e., the layer sintered in an atmosphere of N_2O was at the periphery of the core. The layers had an identical thickness. We believe that the nitrogen concentration in the glass did not exceed 0.1 % [3].

In the UV spectral region, an absorption spectrum typical of the germanosilicate glass was observed. The cut-off wavelengths for these fibres and the absorption coefficients at 242 nm are presented in Table 1. One can see that the preforms (and fibres) sintered in the nitrogen atmosphere have nearly the same GODC concentration, whose value, however, is certainly higher than for the standard preform No. 909. Fig. 1 shows the profiles of the refractive index and concentration of GODC expressed in terms of the absorption coefficient at 242 nm for preforms Nos 916 and 917 with a double-layer core. Each layer covers half the radius of the preform, and hence one can easily see that both profiles have peaks in the layers sintered in the nitrogen atmosphere.

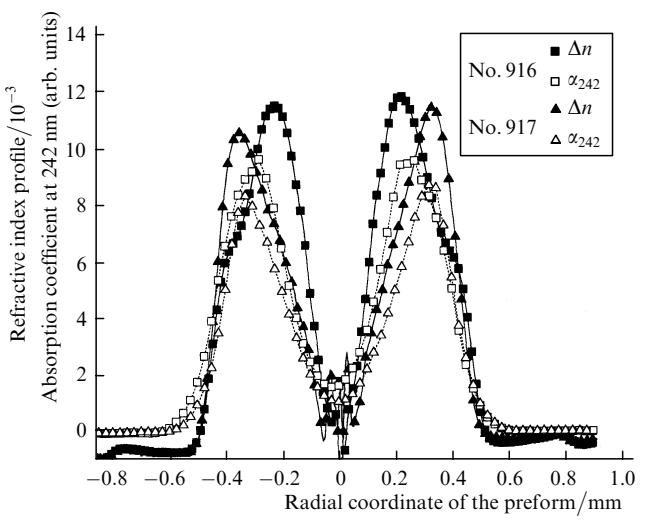

Figure 1. Core–cladding refractive index and absorption coefficient ($\lambda = 242$ nm) profiles for preforms Nos 916 and 917 with a double-layer core. The lines are drawn (here and in the remaining figures) to connect experimental points for a better visual presentation.

3. Experimental results

We studied the photoinduced second harmonic (SH) generation in the fibres prepared. The standard technique was adopted for recording the $\chi^{(2)}$ grating: the fibre was illuminated simultaneously at 532 nm and by IR radiation at 1064 nm. A *Q*-switched mode-locked Nd : YAG laser was used. The pulse duration was 100 ps for a pulse repetition rate of 76 MHz. The pulse train envelope duration was 200 ns, and a pulse train repetition rate was 1.2 kHz. Fig. 2 shows a typical increase in $\chi^{(2)}$ with increasing absorbed radiation energy at 266 nm. This dependence was obtained with the help of our model [2, 6] according to which GODCs are excited by the UV radiation generated inside the fibre during the nonlinear process of mixing of waves at the cubic nonlinear susceptibility $\chi^{(3)}$ ($4\omega = \omega + \omega + 2\omega$). The dependence of $\chi^{(2)}$ on the radiation dose was calculated by using the theoretical values of the 266-nm radiation intensity according to the procedure described in Ref. [2].

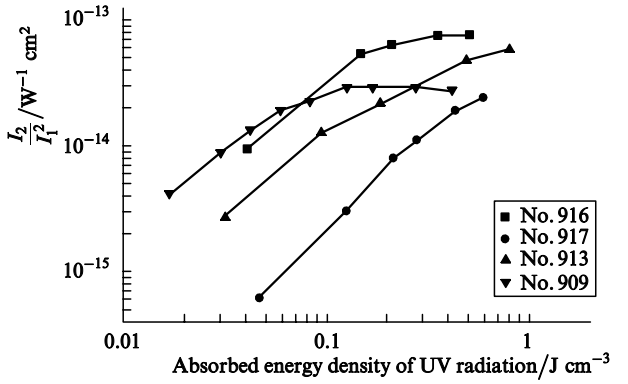

Figure 2. Typical growth of the $\chi^{(2)}$ grating in fibres Nos 916, 917, 913 and 909 as a function of the absorbed energy density of radiation at 266 nm. The peak power of first harmonic radiation during recording was $P_1 = 10 - 11$ kW, of the probing second harmonic $P_2 = 60 - 70$ W, I_1 is the peak intensity of the IR radiation during reading, and I_2 is the peak intensity of the photoinduced SH.

Fibre No. 916 (with the inner layer sintered in an atmosphere of N_2O) had the highest efficiency of recording of the $\chi^{(2)}$ grating among all the fibres under identical conditions of irradiation. On the contrary, fibre No. 917 (with the peripheral layer sintered in an atmosphere of N_2O) displayed an even lower efficiency of recording than the pure germanosilicate fibre No. 909.

In order to find the difference in the efficiencies of photocentres for samples with a double-layer core, we recorded the photoinduced SH with a 20 μm step over the diameter in plates cut out of preforms Nos 916 and 917 (Fig. 3). The intensity profile of the SH recorded is shown in Fig. 3 and is in good agreement with the absorption profile measured at 242 nm (see Fig. 1). Thus, nitrogen-containing layers having a maximum concentration of GODCs are found to be the most photosensitive in both samples.

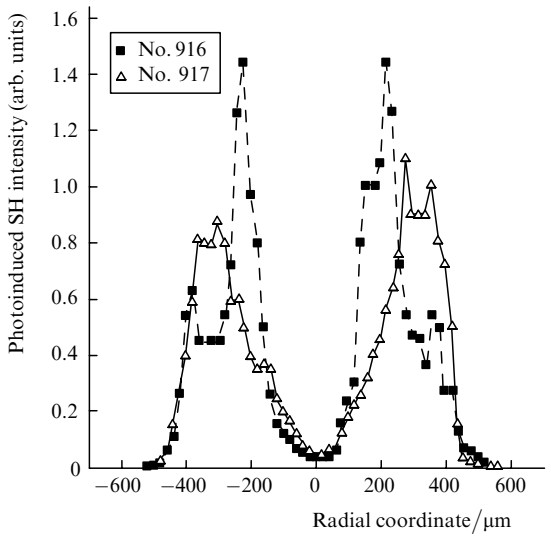

Figure 3. Radial distribution of the intensity of photoinduced SH in preforms Nos 916 and 917 (sample thickness 110 μm); IR radiation at 1064 nm and probing radiation at 532 nm (peak powers of 14 kW and 240 W, respectively) were focused on the preform with the help of 20× objectives, and the recording time was 1 min.

In order to determine the role played by the modification of GODCs by nitrogen in this series of samples, we irradiated the samples (half the preforms) successively with different doses of the ArF laser radiation at 193 nm. After each dose, the photoinduced SH was recorded under identical conditions over the sample diameter (Fig. 4).

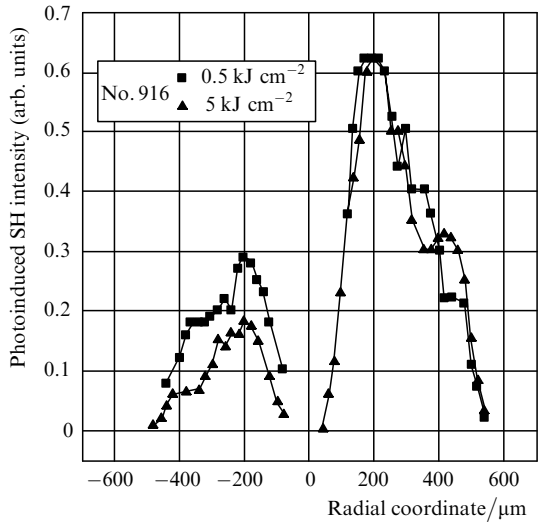

Figure 4. Radial distribution of the intensity of photoinduced SH in preform No. 916. Before each scanning by the photoinduced SH, half the core of the preform (corresponding to the negative scale of distances to the left of the centre of the preform in this figure and in Fig. 7) was exposed preliminarily to radiation at 193 nm (total doses of 0.5 and 5 kJ).

Upon an increase in the radiation dose at 193 nm (in the interval 1 J cm^{-2} – 5 kJ cm^{-2}), the intensity of the photoinduced SH decreased in the irradiated part of the sample. The intensity in the irradiated part of the preforms was higher than in the unexposed part of the sample for low radiation doses (less than 100 J cm^{-2}), and lower for doses exceeding 500 J cm^{-2} (Fig. 5). The loss of photosensitivity (twofold for a radiation dose of 500 J cm^{-2} and fourfold for doses of 5 kJ cm^{-2}) was nearly identical in samples Nos 916 and 917. In each sample, the photoinduced SH profile did not vary significantly upon irradiation. This can be verified, for example, from Fig. 4 showing the profiles of the photoinduced SH for sample No. 916 before and after irradiation. Since the photocentres in layers sintered in atmospheres of nitrogen and oxygen respond identically to irradiation, it can be concluded that only an insignificant number of such centres could have been modified by nitrogen. Hence, the basic reason behind the variation of photosensitivity that should be associated with nitrogen in this series of samples is an increase in the GODC concentration during sintering in the nitrogen atmosphere.

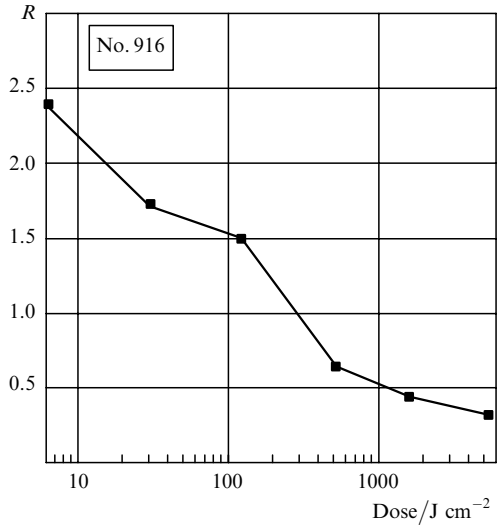

Figure 5. Photoinduced SH intensity in preform No. 916 as a function of the radiation dose at 193 nm; R is the ratio of intensities of photoinduced SH in the exposed part of the preform to its intensity in the unexposed part, averaged over the profile of the preform.

It should be interesting to compare this result with the variations in the absorption spectrum observed after exposing the sample to radiation at 193 nm (Fig. 6). An increase in absorption in the bands at 200, 213 and 281 nm (which are traditionally attributed to GeE', Ge(2), and Ge(1) centres) accompanied by a simultaneous photobleaching of the 242-nm band (GODC) indicates that for doses corresponding to photoinduced variations in the refractive index right up to $\Delta n = 10^{-3}$, radiation at 193 nm produces a large number of positive and negative charges. Because of a high optical density of the samples whose minimum thickness was determined by the conditions of the $\chi^{(2)}$-grating recording, it was difficult to determine the exact concentration of these centres from the magnitude of absorption in the appropriate bands. However, the spectra presented in Fig. 6 enabled us to estimate that the concentration of GeE' and Ge(2) centres (with which we associate the positive charge) and of the negatively charged Ge(1) centres are $(1 - 10) \times 10^{18}$ cm^{-3}. The saturation of the absorption in the region of the band corresponding to the Ge(1) centres for doses exceeding 500 J cm^{-2} is worth noting.

One can see from Fig. 7 that there are significant differences in the radial absorption profiles at 200 nm (GeE') and 270 nm [Ge(1)] after irradiation. While the

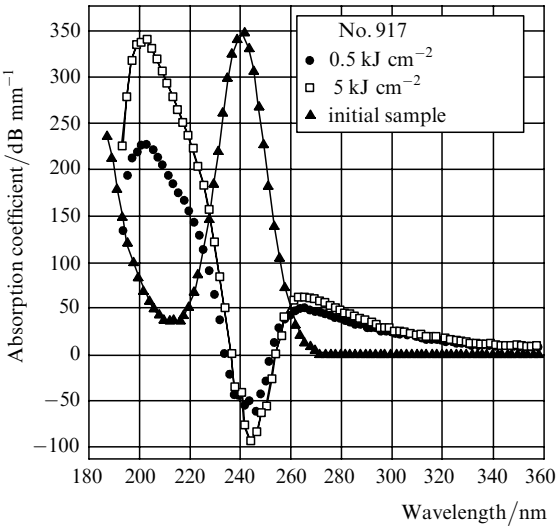

Figure 6. Initial and induced ($\lambda = 193$ nm) absorption in preform No. 917 (sample thickness 110 μm) for various radiation doses. The induced absorption spectrum was normalised to an effective penetration depth d of radiation at 193 nm ($d = 1/\alpha_{193} = 26$ μm).

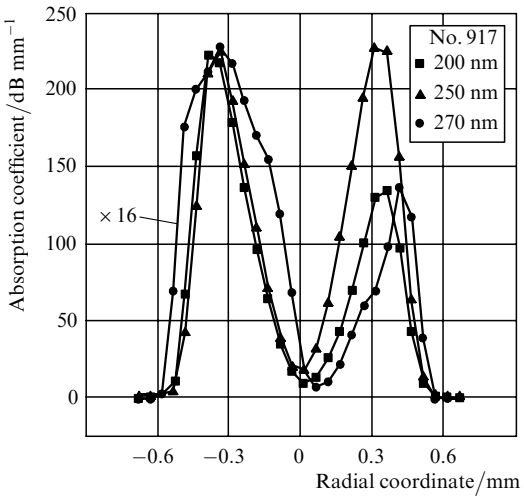

Figure 7. Radial distribution of absorption at 200, 250 and 270 nm after exposure of half the core of preform No. 917 to radiation at 193 nm (dose 0.5 kJ cm^{-2}). The plot for 270 nm is stretched by a factor of 16.

former virtually coincides with the profile of the initial GODCs, the latter is found to be much broader. The broadening of the absorption profile at 270 nm points towards the possibility of charge separation as a result of diffusion of photoelectrons produced during the photoionisation of the initial GODCs.

We also recorded the Δn grating in fibres with a double-layer core by using the 244-nm SH from a cw Ar^+-laser. The induced refractive index was measured by the interferometric technique [7]. As in the case of recording of the photoinduced SH, the recording efficiency of Δn_{ind} in fibre No. 916 was higher (Fig. 8). Earlier, we had observed [2] a correlation in the efficiency of recording Δn and $\chi^{(2)}$ gratings in germanosilicate fibres with different impurity concentrations.

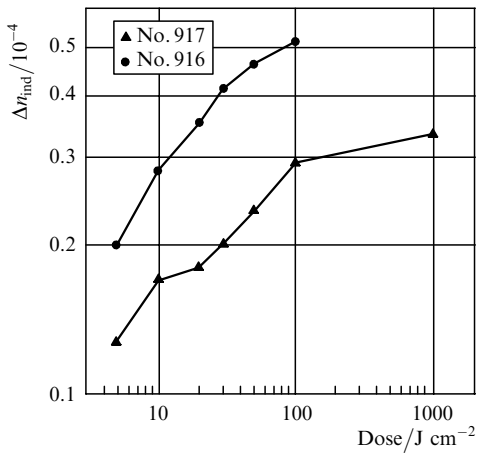

Figure 8. Photoinduced variation of the refractive index measured in single-mode fibres Nos 916 and 917 with the help of an interferometer formed by two long-period gratings, as a function of the exposure radiation dose at 244 nm. The radiation intensity was 10 W cm^{-2}.

4. Discussion

We believe that the results presented in this work reflect the role of the distribution of germanium donors (GODCs) and traps [four-coordinated germanium, which forms a Ge(1) centre during the capture of a photoelectron] in the formation of $\chi^{(2)}$ and, perhaps, Δn gratings. An increase in the photosensitivity of germanosilicate fibres with impurities like nitrogen may be due not only to direct involvement of this impurity in the charge transport processes. The role of nitrogen in increasing the GODCs concentration and the creation of a favourable radial distribution of GODCs and germanium traps during the synthesis of preforms is more important from the point of view of charge separation. It follows from our results that a favourable distribution means a relative increase in the concentration of GODC donors at the centre of the core and an increase in the concentration of traps near the boundary between the core and the cladding. A strong influence of the radial distribution of the photocentres indicates that the coherent photocurrent model [8] is appropriate for describing the mechanism of formation of the $\chi^{(2)}$ grating. (This model is based on the concept of a large-scale spatial charge separation whose size is comparable with the transverse dimensions of the fibre mode.)

Within the framework of this model, let us evaluate the electrostatic field forming the $\chi^{(2)}$ grating for double-layer core fibres with identical layer thickness and an ideal separation of donors and traps in the layers.

In the coherent photocurrent model, the saturation value of the $\chi^{(2)}$-grating amplitude and the electrostatic field $E = \chi^{(2)}/3\chi^{(3)}$ is determined by equating the coherent photocurrent j_{coh} and the conduction current j_{cond}. While writing the expression for the coherent photocurrent, we take into account the fact that it is responsible for an asymmetric radial charge separation due to photoionisation of GODCs. Therefore, it must depend on the overlap integral of the radial distribution of the GODC concentration and the cross section of the UV radiation ionising these centres. Note that the reverse conduction current $j_{cond} = \sigma E$ emerges as a result of photoionisation of filled Ge(1) traps formed during an asymmetric charge separation

and must depend on the overlap integral of the UV radiation cross section and the radial distribution of the concentration of the four-coordinated germanium (GeO_2), which is a precursor of Ge(1). In this case, the electrostatic field $E = j_{coh}/\sigma$ at the saturation stage has the form

$$E = \frac{\beta_1 N^{exc}_{GODC}(f_d, I_{UV}, N_{GODC}) I_\omega I^{1/2}_{2\omega} \cos(\Delta k z)}{\sigma_1 N^{ph}_{Ge(1)}(f_{tr}, I_{UV}, N_{GeO_2})}.$$

Here, β_1 and σ_1 are the photovoltaic constants; I_ω and $I_{2\omega}$ are the intensities of the IR radiation and of the seed second harmonic during the recording of the $\chi^{(2)}$ grating; $\Delta k = 2(\omega/c)(n_{2\omega} - n_\omega)$; n_ω and $n_{2\omega}$ are the refractive indices of the fibre core at the frequencies of the IR radiation and its second harmonic, respectively; ω is the IR radiation frequency; z is the axial coordinate; $N^{exc}_{GODC}(f_d, I_{UV}, N_{GODC})$, $N^{ph}_{Ge(1)}(f_{tr}, I_{UV}, N_{GeO_2})$ are the concentrations of the excited GODC and photoionised Ge(1) as functions of the UV radiation intensity I_{UV}, concentrations of their precursors N_{GODC} and N_{GeO_2} the overlap integrals f_d and f_{tr}, respectively.

As in our previous publications [2, 6], we assume that during the $\chi^{(2)}$ grating recording, photoionisation of GODCs occurs as a result of a two-stage process. In the beginning, the fourth harmonic 266-nm UV radiation generated inside the fibre in a nonlinear process at $\chi^{(3)}$ ($4\omega = \omega + \omega + 2\omega$) excites GODCs to the singlet (S_1) and triplet (T_1) levels. After this, these centres are photoionised from their excited levels by IR radiation at 1064 nm in a two-photon process and by its second harmonic at 532 nm in a one-photon process. The interference of these two photoionisation channels generates an asymmetric coherent photocurrent that forms a periodic electrostatic field and the structure of the $\chi^{(2)}$ grating. We assume that at the saturation stage, almost all photoionised electrons are located in Ge(1) traps. We also assume that the 266-nm radiation falling in the 281-nm absorption band of Ge(1) centres makes the main contribution to the photoionisation of Ge(1) in a single-photon process.

Then, assuming that the radial distributions of the donor and trap concentrations are described by Gaussians, we can represent the electrostatic field in the form:

$$E = \frac{\beta_1 f_1 N_{GODC} I_\omega I^{1/2}_{2\omega} \cos(\Delta k z)}{\sigma_1 f_2 N_{Ge(1)}},$$

where N_{GODC} and $N_{Ge(1)}$ are the concentrations of the donors and the filled traps at the maxima of their radial distributions: $f_1 = \exp[-2\Delta r_d^2/(w_{4\omega}^2 + w_d^2)]$; $f_2 = \exp[-2\Delta r_{tr}^2/(w_{4\omega}^2 + w_{tr}^2)]$; Δr_d, w_d and Δr_{tr}, w_{tr} are the radial displacements of the concentration peaks relative to the fourth harmonic Gaussian mode and half-widths of the radial distribution of concentrations of GODCs and Ge(1), respectively; and $w_{4\omega}$ is the half-width of the Gaussian mode for the fourth-harmonic radiation.

In the case of an initially homogeneous distribution of GODCs and GeO_2 centres [precursors of Ge(1) centres], the radial distribution of the photoionised donors coincides with the fourth harmonic Gaussian mode, while the maximum of the distribution of Ge(1) centres is displaced towards the periphery of the beam in a direction determined by the polarisation of the interfering photoionising radiation. Because the photoionisation of traps is a single-photon process and the electrons are under identical conditions in the conduction band, the radial profile of Ge(1) centres at the saturation stage will repeat the profile of photoionised GODCs. As a result of numerous photoionisation and recombination events, the displacement of the Ge(1) distribution maximum will be nearly equal to the half-width of the fourth harmonic Gaussian mode ($\Delta r_d \approx 0$, $w_d \approx w_{4\omega}$, $\Delta r_{tr} \approx w_{4\omega}$, $w_{tr} \approx w_{4\omega}$ and $f_1/f_2 = e^1$).

We assume that the maximum of the donor concentration in fibres with a double-layer core lies in the inner layer, while the maximum of the concentration of traps lies in the peripheral layer. The cross section of the fourth harmonic Gaussian mode formed in the nonlinear process with an intensity $I_{4\omega} \sim (\chi^{(3)} l)^2 I^2_\omega I_{2\omega}$ (l is the coherence length) virtually coincides with the inner layer in size ($w_{4\omega} = w_\omega/\sqrt{3}$, where w_ω is the half-width of the Gaussian cross section of the lowest fibre mode in which the IR radiation propagates). In this case, $w_d \approx w_{4\omega}$, $\Delta r_d \approx 0$, $w_{tr} \approx w_{4\omega}$, $\Delta r_{tr} \approx 2w_{4\omega}$, $f_1/f_2 \approx e^4$ and the electrostatic field increases compared to the homogeneous distribution by a factor of $E_{NU}/E_U = e^3 \approx 20$. If the donor and trap concentration maxima are arranged in the opposite order in the fibre layers, we have $w_d \approx w_{4\omega}$, $\Delta r_d \approx 2w_{4\omega}$, $w_{tr} \approx w_{4\omega}$, $\Delta r_{tr} \approx w_{4\omega}$, $f_1/f_2 \approx e^{-3}$ and the decrease in the electrostatic field compared to the homogeneous distribution is by a factor of $E_{NU}/E_U = e^{-4} \approx 0.02$.

The difference in the efficiencies of recording of the photoinduced SH was much smaller in our experiments with fibres Nos 916 and 917 with a double-layer core [$(I_2)_{916}/(I_2)_{917} = (\chi^{(2)}_{916})^2/(\chi^{(2)}_{917})^2 = 3.1$]. One can see from Fig.1 that the distribution $\Delta n(r)$ in preforms with a double-layer core has a large dip in the middle, and the profiles of the refractive index and absorption of GODCs differ insignificantly. Our analysis of the profiles of refractive index and absorption of GODCs measured in samples Nos 916 and 917 (Fig. 1) showed that theoretical ratios of the SH intensities were quite close to the experimental values [$(f_1/f_2)_{916} \approx e^{0.696}$, $(f_1/f_2)_{917} \approx e^{0.171}$, $E_{916}/E_{917} = 1.69$ and $(\chi^{(2)}_{916})^2/(\chi^{(2)}_{917})^2 = 2.9$].

Thus, a considerable increase in the electrostatic field in fibres with a double-layer core can be attained only if the core has a more pronounced separation of the inner layer (sintered in nitrogen atmosphere) containing the GODC concentration maximum and the peripheral layer (sintered in oxygen atmosphere) containing the GeO_2 concentration maximum. We believe that the desired result could be attained through a precise control over the concentration of chlorides and the temperature at various stages of the technological process.

The increase in the intensity of the photoinduced SH after exposure to UV radiation that we observed in preforms for small radiation doses (193 nm) is an expected result. In earlier publications [9, 10], an increase was reported in the SH efficiency after preliminary exposure of the fibres to radiation at 266 nm [9] and 351.1 nm [10]. Since the extent of GODC damage by radiation at these wavelengths is much smaller than by the radiation at 193 nm, the radiation doses used in these works (radiation power 0.1 – 1 mW, exposure time tens of seconds) correspond to very small doses of radiation at 193 nm. The most likely reason behind an increase in SH for small UV radiation doses is the emergence of an auxiliary channel of charge transport by a coherent photocurrent, i.e., photoionisation and reorientation of Ge(1) traps generated by radiation at 193 nm. Photoionisation of Ge(1) centres by radiation at 266 nm is

quite efficient [11], and hence the total effective photoelectric constant for coherent photocurrent will be higher than in the unirradiated sample.

It was shown in experiments using KrF-laser radiation at 248 nm that the concentration of Ge(1) centres attains saturation for radiation doses $1-10$ J cm^{-2} [11, 12]. For higher doses, damage of GODCs occurs with the predominant formation of GeE' centres [13]. The damage of GODC centres in this case may take place through a structural rearrangement without photoionisation [14]. Thus a decrease in the intensity of photoinduced SH following large doses of radiation at 193 nm may be attributed to a loss of the GODC photoionisation efficiency due to a decrease in the concentration of donor centres and saturation of the induced Ge(1) centres, which may be reoriented.

As far as the mechanism of formation of Δn grating is concerned, it is also interesting to note that for typical total radiation dose at 193 nm used for Δn recording (several kJ cm^{-2}), the damage of GODCs is followed by the emergence of more than 10^{18} cm^{-3} positive and negative charges, which are separated in space because of an inhomogeneous distribution of GODCs. A considerable broadening (of the order of 100 μm) of the profile of this band observed in preforms may be attributed to the GODC concentration gradients produced by small-scale (of the order of 1 μm) inhomogeneities in germanosilicate glass, which cannot be seen in Figs 1 and 7 [15]. In fibres with an inhomogeneous impurity distribution, the GODC concentration gradients increase roughly by two orders of magnitude compared to those measured in the preforms, and the role of spatial charge separation in initiating the processes of structural rearrangement at the final stage of the Δn-grating formation may become quite significant.

A more efficient recording of $\chi^{(2)}$ and Δn gratings in the same fibre with a double-layer core may also reveal the effect of GODCs and charge separation on the formation of Δn. However, the absorption profiles of GODCs and GeO_2 do not differ significantly in the samples prepared by us. Therefore, it is quite possible that the final form of the photoinduced Δn profile may be determined by photoprocesses that depend on the Ge concentration and are not related to charge separation.

The question of correlation of the optimal radial distribution of GODCs and GeO_2 in the recording of Δn and $\chi^{(2)}$ gratings requires further investigations and, among other things, the preparation of samples with a better separation of germanium donor and acceptor centres.

5. Conclusions

In the series of germanosilicate preforms and fibres doped inhomogeneously with nitrogen prepared by us, the efficiency of the Δn and $\chi^{(2)}$-grating recording is found to depend on the radial distribution of photocentres. A threefold increase in the intensity of photoinduced SH obtained in a fibre with a double-layer core is caused by the redistribution of GODCs and germanium traps rather than by a modification of photocentres by nitrogen. It is shown that this intensity can be increased significantly by separating germanium donor and acceptor centres more distinctly at the stage of preparation of preforms.

A decrease in the photoinduced SH following large radiation doses at 193 nm suggests the damage of GODCs due to structural rearrangement without photoionisation.

The strong absorption bands observed for Ge(1), Ge(2) and GeE' centres, which have different widths over the radius of the preforms for the 193-nm radiation doses typical of the photorefractive effect suggest a high (more than 10^{18} cm^{-3}) concentration of positive and negative charges and indicate to the possibility of a significant role of charge separation in initiating the processes of Δn-grating formation at the final stage.

Acknowledgements. The authors thank V.B. Neustruev for the support of this work and critical remarks. This work was supported by the Russian Foundation for Basic Research (Grant Nos 01-02-17751 and 00-15-96650).

References

1. Dianov E.M., Golant K.M., Mashinsky V.M., Medvedkov O.I., Nikolin I.V., Sazhin O.D., Vasiliev S.A. *Electron. Lett.*, **33**, 1334 (1997).
2. Dianov E.M., Guryanov A.N., Khopin V.F., Mashinsky V.M., Medvedkov O.I., Sazhin O.D., Vasiliev S.A., Vechkanov N.N., Yatsenko Yu.P. *Proc. SPIE Int. Soc. Opt. Eng.*, **4083**, 144 (2000).
3. Sulimov V.B. *Doct. Diss.* (Moscow, General Physics Institute, Russian Academy of Sciences, 1997).
4. Saifi M.A., Andrejco M.J. *Opt. Lett.*, **13**, 773 (1988).
5. Dong L., Pinkstone J., Russell P.St.J., Payne D.N. *J. Opt. Soc. Am. B*, **11**, 2106 (1994).
6. Dianov E.M., Kornienko L.S., Yatsenko Yu.P. *Kvantovaya Elektron.*, **23**, 652 (1996) [*Quantum Electron.*, **26**, 636 (1996)].
7. Dianov E.M., Vasiliev S.A., Kurkov A.S., Medvedkov O.I., Protopopov V.N., in *Proc. ECOC'96* (Oslo, Norway, 1996) Vol. 1, p. 65.
8. Dianov E.M., Kasansky P.G., Krautschik C., Stepanov D.Yu. *Sov. Lightwave Commun.*, **1**, 381 (1991).
9. Carvalho I.C.S., Margulis W. *Opt. Lett.*, **16**, 1487 (1991).
10. Driscoll T.J., Lavandy N.M. *Opt. Lett.*, **17**, 571 (1992).
11. Neustruev V.B., Dianov E.M., Kim V.M., Mashinsky V.M., Romanov M.V., Guryanov A.N., Khopin V.F., Tikhomirov V.A. *Fibers and Integrated Optics*, **8**, 143 (1989).
12. Fujimaki M., Yagi K., Okhi Y., Nishikava H., Awazu K. *Phys. Rev. B*, **53**, 9859 (1996).
13. Nishii J., Fukumi K., Yamaka H., Kawamura K., Hosono H., Kawazoe H. *Phys. Rev. B*, **52**, 1661 (1995).
14. Essid M., Albert J., Brebner J.L., Awazu K. *J. of Non-Cryst. Solids*, **246**, 39 (1999).
15. Dianov E.M., Mashinsky V.M., Neustruev V.B., Sazhin O.D., Guryanov A.N., Khopin V.F., Vechkanov N.N., Lavrishchev S.V. *Opt. Fiber Technology*, **3**, 77 (1997).